Features of the 4-dimethylaminobenzoylhydrazone ethyl ester of 2.4-dioxopentanoic acid

Bako B. Umarov[1], *Murod A.* Tursunov[1], *Jamshid M.* Ashurov[2], *Ne'mat G.* Sevinchov[1], *Maftuna J.* Ruzieva[1], *Dilobar N.* Sevinchova[3], *Bakhtiyor Sh.* Ganiev[1*], and *Furkat N.* Khayrullayev[1]

[1]Bukhara State University, M. Ikbol 11, Bukhara, 200117, Uzbekistan
[2]Institute of Bioorganic Chemistry, Uzbekistan Academy of Sciences, M. Ulugbek Str., 83, Tashkent, 100125, Uzbekistan
[3]Bukhara State Medical Institute named after Abu Ali ibn Sina, 200118, Gijduvan str., 23, Bukhara, Uzbekistan

Abstract. The composition and structure of 4-dimethylaminobenzoylhydrazone ethyl ester of 2,4-dioxopentanoic acid (I) were established by elemental analysis, IR and 1H-NMR spectroscopy. The resulting ligand single crystals were studied by X-ray diffraction analysis. Thus, as a result of IR, NMR-1H, and X-ray studies, it was found that the compound I in the solid state is in the pyrazoline ring IC. In the crystal structure, the organic molecules are linked with the intermolecular O–H···O, C–H···O hydrogen bonds as well as C–H··· π and π–π interactions which form 3D crystal structures and ensure the lattice stability. Hirshfeld surface analysis indicates that the most important contributions to the crystal packing stem from H…H (58.2%), H…O/O…H (19.5%) and H…C/C…H (14.9%) interactions. Energy framework calculations reveal a significant contribution of dispersion energy. The calculated highest occupied molecular orbital (HOMO) and lowest unoccupied molecular orbital (LUMO) energy gap is 4.522 eV.

1 Introduction

Acyl- and benzoylhydrazones of 1,3-diketones represent an extremely interesting class of compounds with respect to tautomeric capabilities, attention to which is constantly growing [1-2]. The interest in the fine structure of acylhydrazones is primarily due to the fact that they are capable of being in various tautomeric forms. Depending on the structural features of the dicarbonyl component in the series of acylhydrazones of 1,3-diketones, a triple ring chain equilibrium can be expected between linear (hydrazone, enhydrazine) and cyclic 5-hydroxy-2-hydroxypyrazoline tautomeric forms. It should be noted at once that paired prototropic equilibrium was observed for acylhydrazones of both 1,3-ketoesters and 1,3-ketoaldehyde derivatives. We have studied the structure of condensation products of 2,4-

* Corresponding author: b.ganiyev1990@gmail.com

dioxopentanoic acid (I) ethyl ether with hydrazides of para-substituted aromatic acids [3]. We report herein the synthesis, crystal structure and Hirshfeld surface analysis for a new ethyl ester of 2,4-dioxopentanoic acid derivative, 4-dimethylaminobenzoylhydrazone ethyl ester of 2,4-dioxopentanoic acid.

Judging by the NMR-^{1}H spectroscopy data, the free 1,3-ketoester, namely, the ethyl ether of 2,4-dioxopentanoic acid is in the keto-enol form. The composition and structure of the obtained acylhydrazones (II) based on ketoether (I) was determined by elemental analysis, IR and NMR-^{1}H spectroscopy.

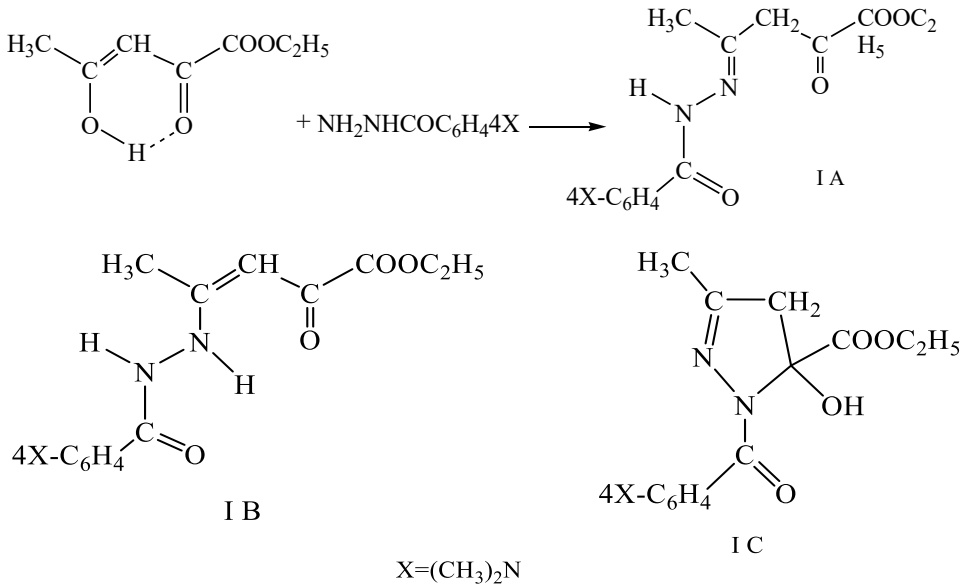

Fig. 1. Chemical diagram of synthesis *para*-dimethylaminobenzoylhydrazone ethyl ester of 2,4-dioxopentanoic acid (I).

2 Experimental part

2.1 Materials and methods

The organic solvents and other agents used in the work were purified and dried according to [4-6]. Analysis of C, H and O were performed on a German Elementar Vario EL instrument. IR absorption spectra were recorded on Nicolet UR-20, Specord 75IR, Perkin Elmer FT-IR, and AVATAP-360 spectrometers in the range 400–4000 cm^{-1} in KBr pellets [7-8]. NMR-^{1}H spectra of 5-10% ligand solutions were recorded on Tesla-BS-497 (100 MHz), XL-100 (Varian) (100 MHz), Bruker DPX-300 (300.13 MHz) and Unity 400 plus spectrometers. (Varian). NMR-^{13}C spectra were recorded on a CFT-20 (20 MHz) and Bruker DPX-300 (75 MHz) instrument for saturated solutions in a pulsed mode with a Fourier transform under conditions of monoresonance and noise decoupling from protons [9].

2.2 Synthesis and crystallization

Synthesis of 4-dimethylaminobenzoylhydrazone of 2,4-dioxopentanoic acid ethyl ester (Fig. 1).

To a solution of 0.948 g (0.006 mol) of 2,4-dioxopentanoic acid ethyl ester in absolute ethanol was added a solution of 1.074 g (0.006 mol) of para-dimethylaminobenzoylhydrazine in absolute ethanol, and the reaction mixture was kept at 20-25°C. The reaction progress was monitored by TLC on Silufol UV-254 plates (eluent $CHCl_3$). At the end of the reaction, the solvent was removed on a rotary evaporator. 1.26 g of 2,4-dioxopentanoic acid ethyl ester *para*-dimethylaminobenzoylhydrazone was obtained. Yield: 65%. Elemental analysis for $C_{16}H_{21}N_3O_4$ (Mr=319.36): calculated: C 60.18; H 6.58; N 13.16%; found: C 60.25; H 6.49; N 13.15%.

2.3 X-ray structure analysis and refinement

Data for the crystal structure determinations were collected on an Oxford Diffraction Xcalibur-R CCD diffractometer (CuKa –radiation, = 1.54184 Á, (ω-scan mode, graphite monochromator (at 293K) [10]. The structure was solved and refined using program packages *SHELXT2014/5* and *SHELXL2016/6* [11]. All non-hydrogen atoms were refined anisotropically. Hydrogen atoms were inserted at calculated positions and constrained with isotropic thermal parameters. The molecular drawings were plotted by MERCURY program package [12]. The crystallographic data and details of the structure refinement are given in Table 1. Crystallographic data have been deposited with Cambridge Crystallographic Data Centre (Deposite Number 2173511). The data can be obtained free of charge via http://www.ccdc.cam.ac.uk/conts/ retrieving.html or from the Cambridge Crystallographic Data Centre, 12 Union Road, Cambridge CB2 IEZ, UK; fax: (+44) 1223-336-033; or e-mail: deposit@ccdc.cam.ac.uk.

Table 1. The crystal data and structure refinement details.

Formula	$C_{16}H_{21}N_3O_4$
Formula weight	319.36
Crystal system	triclinic
Space group	*P-1*
a, Å	7.9240(11)
b, Å	8.2192(9)
c, Å	13.987(2)
α, deg	81.081(11)
β, deg	81.940(12)
γ, deg	62.199(13)
V, Å^3	793.7(2)
Z	2
D_x, g cm^{-3}	1.336
$\mu(CuK_\alpha)$, mm^{-1}	0.803
Crystal size [mm]	0.16 x 0.28 x 0.38
T, K	293
Scan θ range, deg	3.2, 76.0
Range *h,k,l*	-9/9; -7/10; -17/17
Total data	5166
Independent data	3181
R_{int}	0.045
Observed data [$F^2 \geq 2\sigma(F^2)$]	2220
Refined parameteres	217
Goodness-of-fit (F^2)	1.20
R_1, $wR_2(I>2\sigma(I))$	0.0912, 0.3108
$\Delta\rho_{min/max}$, *e*Å^{-3}	-0.29/0.34

2.4 Hirshfeld surfaces calculations

Hirshfeld surfaces and fingerprint plots were calculated for the title compound based on the crystallographic information file (CIF) using the CrystalExplorer program [13]. The 2D fingerprint plots displayed by using the standard 0.6-2.6 Å view with the d_e and d_i distance scales displayed on the graph axes. Hirshfeld surfaces were obtained using a standard (high) surface resolution with the three-dimensional d_{norm} surfaces mapped over a fixed color scale of -0.777 (red) to 1.273 (blue). Points with a contribution to the Hirshfeld surface are coloured by blue color for a small contribution and through green to red for points with the greatest contributions.

2.5 DFT calculation method

Theoretical calculations were carried out by the hybrid density functional theory method (DFT) - B3LYP using Aldrich's def2-TZVP basis set. Input file for the DFT calculations in ORCA 4.2.0 [14] program package generated by Avogadro [15] program package using X-Ray determined geometry (cif file). The calculations results analyzed by Avogadro and Multiwfn [16] program packages.

3 Results and discussion

3.1 Description of molecular structure

The molecular structure of the title compound is illustrated in Fig. 2. Five membered heterocyclic pyrazoline rings, consisting of atoms C(1)C(2)C(3)N(2)N(1) flat. The maximum deviation of atoms from the plane of heterocycles is 0.0036–0.0067 Å (H_2L), respectively, and for phenyl rings these deviations are 0.0067 Å. The phenyl ring of the benzoylhydrazide residue in the molecule (H_2L) is rotated relative to the pyrazoline ring in space by 45.66°. The angle between the ester group of the β-diketone part of the molecule and the hydroxypyrazoline ring is 136.42° and they lie outside the same plane, although the ester group itself is sufficiently coplanar, as indicated by the value of the dihedral angle O(1)C(4)O(2)C (5) – 4.38°. An analysis of the bond lengths of the molecule shows that this molecule has double bonds N(2)=C(3) 1.27 Å, O(1)=C(4) 1.20 Å and O(4)=C(8) 1.23 Å. The slight difference between the double bonds O(1)=C(4) and O(4)=C(8) is explained, as was determined above, by the inclusion of the oxygen atom O(4) in the p-π-conjugation by the free pair of the *p*-electron with the π-orbital of the aromatic nucleus.

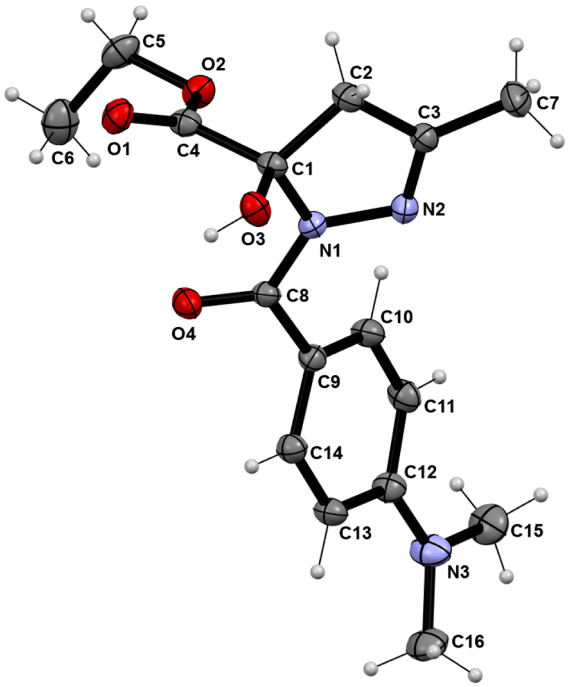

Fig. 2. The view of the asymmetric unit of the title compound I with labeling of basic nonhydrogen atoms.

3.2 Supramolecular features and hydrogen bonds

The packing of structural units in the **I** crystal is shown in Fig. 3. The O–H atomic bond of the hydroxyl fragment of the pyrazoline cycle takes part in the formation of the intermolecular hydrogen bond O(3)–H(3)···O(4) with the benzoyl oxygen atom. Ester ketonium oxygen O(1) forms other molecules of the phenyl fragment C(14) by hydrogen C(14)–H(14A)···O(1) of the intermolecular hydrogen bond, which are added to the mass of the intermolecular dimer: O(3)–H(3) 0,78, H(3)···O(4) 2,07, O(3)–O(4) 2,782 Å, angle N(3)H(3)O(4) 157,1°; C(14)–H(14) 0,93, H(14)···O(1) 2,56, C(14)–O(1) 3,469Å, angle C(14)H(14)O(1) 164° (Table 2).

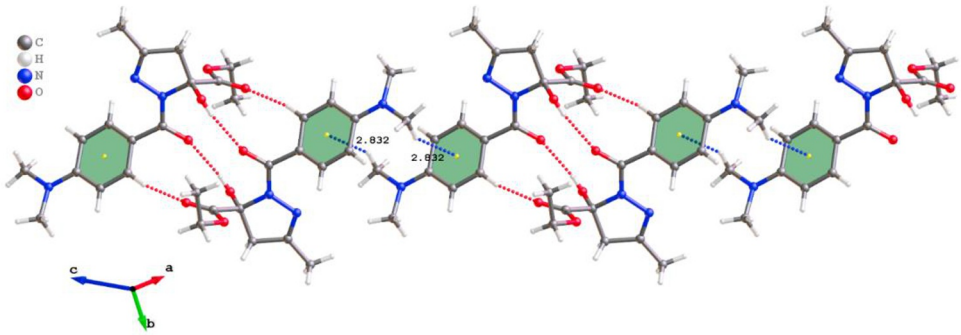

Fig. 3. Packing diagram of **I**. Interactions shown with dotted lines; hydrogen bonds in red and C-H…π interactions in blue.

Table 2. Hydrogen Bonds (Angstrom, Deg).

Bond, D-H···A	D-H, Å	H···A, Å	D···A, Å	∠D-H···A, °
O3-H3···O4^{i}	0.77(9)	2.06(9)	2.781(6)	157(8)
C14-H14···O1^{i}	0.930	2.5600	3.468(7)	164.00

Symmetry code: (i) 1-x, 1-y, 2-z.

3.3 Spectroscopic studies (I)

The band of stretching vibrations of the C=O bond of the ethyl group of the ester fragment of the β-diketone part of the H_2L compound molecule is observed at 1750–1765 cm^{-1}. The IR spectra of these compounds are characterized by a wide band of stretching vibrations in the region of ~3400 cm^{-1} $\nu_{(O-H)}$; In the IR spectra of compounds in the range of stretching vibrations of multiple bonds, there are intense absorption bands in the region of 1633, 1595, 1574, 1558, and 1490 cm^{-1}. The absorption band at 1633 cm^{-1} indicates the presence of the C=N bond, the remaining absorption bands belong to vibrations of one and a half bonds of the aromatic ring and bending vibrations of the N–H bond. Analysis of the IR spectra indicates that the synthesized **I** compounds in the solid state are mainly in the cyclic 5-hydroxy-2-pyrazoline tautomeric form ©.

In order to unambiguously prove the conclusions about the structure of the obtained H_2L compounds, we recorded their NMR-^{1}H spectra in a $CDCl_3$ solution. The spectra indicate the retention of the cyclic tautomeric form (B). As an example, let us consider the NMR-^{1}H spectrum of the compound H_2L taken immediately after the preparation of the solution. Of particular importance is the signals of the protons of the methylene group of the pyrazoline ring as asymmetric doublet signals at δ 2.98-3.03 and 3.17-3.28 ppm, forming a typical AV system with SSCC J_{AB}=21 Hz. This is due to the presence of a chirality center in the molecule, which is the carbon atom in the fourth position of the 5-hydroxy-2-pyrazoline ring [9, 17-19].

The protons of the ethyl group of the β-dicarbonyl part form a characteristic pattern of triplet and quadruplet signals with a ratio of integral intensities of 3:2 at δ 1.28 and a substituent $(CH_3)_2N$ of the 6ydrazine fragment at δ 4.34 ppm, and the protons of the phenyl ring (5H) resonate as a somewhat broadened multiplet signal centered at δ 7.46 and 7.93 ppm. The signal from a single proton of the hydroxyl group associated with the fifth carbon atom of the 5-hydroxy-2-pyrazoline ring for all ligands is observed at δ 7.28 ppm. Substituents in the para-position of the benzene ring of the amide part of the molecule, by their electron-donating or electron-withdrawing nature, strongly affect the chemical shifts of the proton signals of all terminal substituents and functional groups of the molecule, [2, 20-21]. This is especially noticeable for signals from the protons of the aromatic nucleus and the carbon atom in the 4-th position of the pyrazoline ring.

Under the influence of the electron-withdrawing nitro group, the signals of these protons resonate in the region of weaker fields for the compound, the signals of the protons of the benzene ring are shifted for the compound H_2L, where the electron-donating N,N-dimethylamine group is introduced in the *para*-position of the benzene ring, the same signals are shifted in the region of a strong field up to Δ δ 0.75 ppm The discussed research data are in full agreement with the previously obtained results for this class of compounds and are in good agreement with these conclusions [3, 21-25].

Approximately the same changes are observed in a detailed discussion of the assignment of the chemical shifts of the resonant signals of two sterically nonequivalent protons corresponding to the chiral center and forming a typical AB system under the influence of the asymmetric C* atom in position 5 of the hydroxypyrazoline heterocycle.

3.4 Hirshfeld surface analysis

The overall two-dimensional fingerprint plot, Fig. 4a, and those delineated into H···H, H···O/O···H, H···C/C···H, H···N/N···H, C···O/O···C contacts are illustrated in Fig. 4b–f.

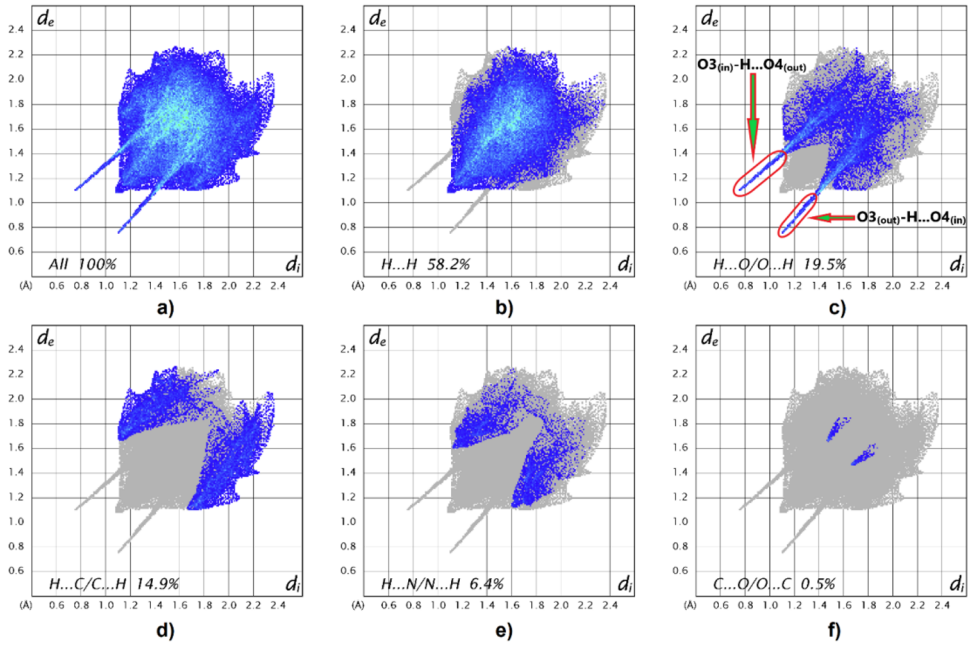

Fig. 4. The full two-dimensional fingerprint plots for the title compound, showing all interactions (a), and delineated into (b) H···H, (c) H···O/O···H, (d) H···C/C···H, (e) H···N/N···H and (f) C···O/O···C interactions. The d_i and d_e values are the closest internal and external distances (in Å) from given points on the Hirshfeld surface.

The d_{norm} plot was estimated via calculations of the external (d_e) and internal (d_i) distances to the nearest nucleus and built over the volume of 389.68 Å^3 and an area of 357.10 Å^2, with scaled colour of -0.5790 (red) a.u. to 1.2968 (blue) a.u. (Fig. 5). The plots of shape-index and curvedness were generated in the range of -1.0000 to 1.0000 a.u. and -4.0000 to 4.0000 a.u., respectively, (Fig. 6a, b).

The most important interaction is H···H contributing 58.2% to the overall crystal packing, which is reflected in Fig. 4b as widely scattered points of high density due to the large hydrogen content of the molecule with the tip at $de + di \approx 2.2$Å. Fig. 5 shows the Hirshfeld surface of the title compound. The respective acceptor and donor atoms showing strong O-H···O, and C-H···O intermolecular hydrogen bonds (for O3-H3···O4 and C14-H14···O1) are indicated as bright red spots on the Hirshfeld surface.

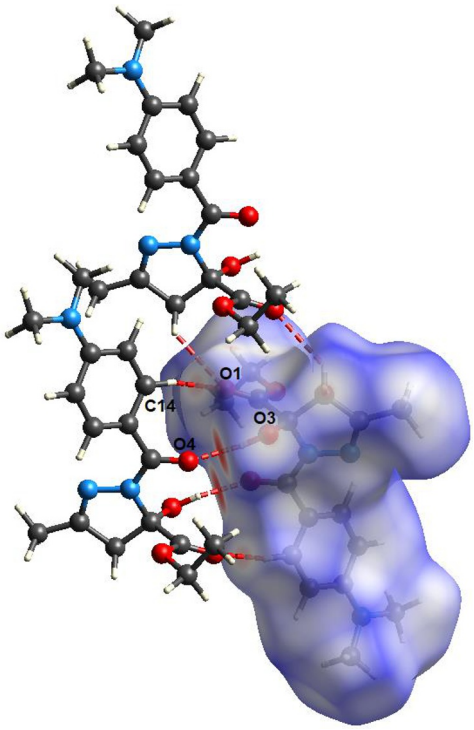

Fig. 5. View of the three-dimensional Hirshfeld surface of the title compound plotted over d_{norm} in the range -0.5790 to 1.2968 a.u. Only labels of the O and C atoms involving in the hydrogen bonds are shown.

This finding is substantiated by the calculated electrostatic potential (Fig. 6d) of the molecule that was used to generate the Hirshfeld surface. The negative potential (acceptor) is indicated as a red surface around the two atoms (O1 and O4) and the blue surface area, indicating the positive potential (donor), is mapped in the proximity of the hydrogen atoms (H3 and H14).

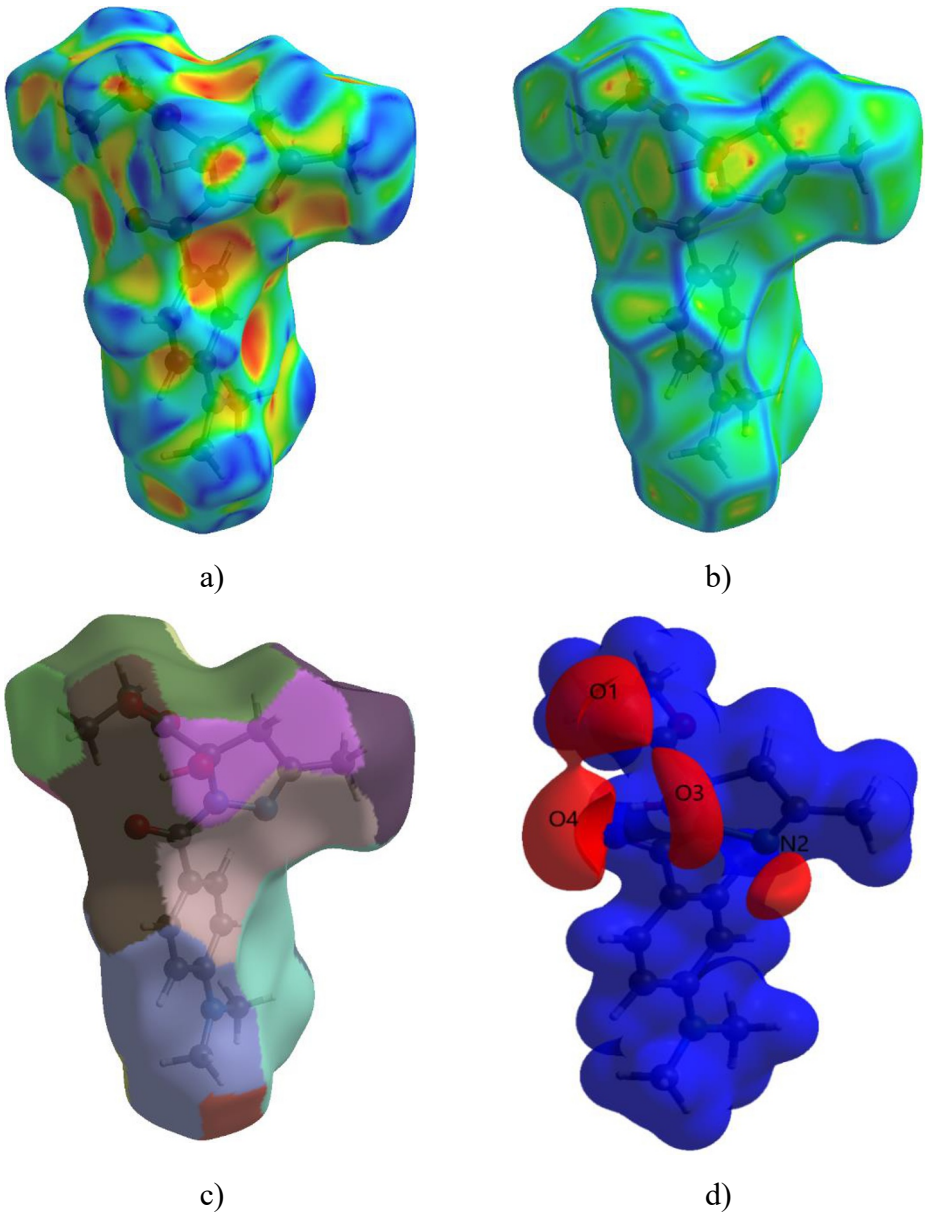

Fig. 6. Hirshfeld surfaces mapped for the shape index (a), curvedness (b), Fragment patch (c) and view of the three-dimensional Hirshfeld surface plotted over electrostatic potential energy in the range-0.0500–0.0500 a.u. using the B3LYP/STO-3G basis set at the Hartree–Fock level of theory. Hydrogen-bond donors and acceptors are shown as blue and red regions around the atoms corresponding to positive and negative potentials, respectively (d).

3.5 Energy framework

Quantification of energy framework energies is considered a powerful method for understanding the topology of the overall interactions of molecules in the crystal. This method allowed us to calculate and compare different energy components, i.e. repulsion

(E_rep), electric (E_ele), dispersion (E_dis), polarization (E_pol) and total (E_tot) energy based on the anisotropy of the topology of pairwise intermolecular interaction energies. CrystalExplorer17.5 (Turner et al., 2017) was used to calculate the energy framework of the title compound by generating new wave functions using the DFT method under 6-31G(d,p) basis set with exchange and potential functions (B3LYP) for a molecular cluster environment for a 111 unit cell. The thickness of the cylinder radius indicates the grade of interactions and is directly related to the energy magnitude and offers information about the stabilization of the crystal packing. In order to avoid the crowdedness of less significant interaction energies, we set the cylindrical radii with a cut-off value of 5 kJ mol (Fig. 7).

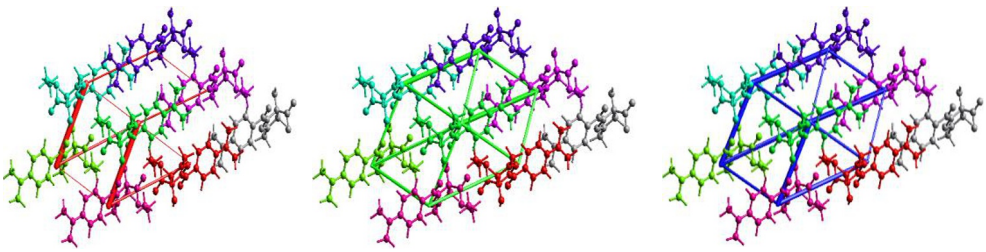

a) b) c)

	N	Symop	R	Electron Density	E_ele	E_pol	E_dis	E_rep	E_tot
	1	x, y, z	7.92	B3LYP/6-31G(d,p)	-3.3	-1.4	-23.8	11.7	-18.0
	0	-x, -y, -z	7.97	B3LYP/6-31G(d,p)	-2.4	-1.3	-31.9	15.8	-21.5
	0	-x, -y, -z	10.79	B3LYP/6-31G(d,p)	-3.3	-1.2	-10.6	7.2	-9.1
	0	-x, -y, -z	10.01	B3LYP/6-31G(d,p)	-22.0	-6.8	-35.0	29.0	-40.8
	1	x, y, z	8.22	B3LYP/6-31G(d,p)	-7.1	-2.5	-22.6	13.7	-20.6
	1	x, y, z	8.34	B3LYP/6-31G(d,p)	-6.8	-1.5	-31.9	14.6	-26.9
	0	-x, -y, -z	12.40	B3LYP/6-31G(d,p)	-7.7	-1.3	-24.5	12.9	-22.4
	1	-x, -y, -z	6.84	B3LYP/6-31G(d,p)	-57.4	-16.0	-28.2	74.4	-51.1
	0	-x, -y, -z	8.51	B3LYP/6-31G(d,p)	0.7	-0.5	-15.4	7.9	-8.2
	1	-x, -y, -z	9.40	B3LYP/6-31G(d,p)	-16.2	-5.4	-52.4	31.3	-47.4
	1	-x, -y, -z	9.56	B3LYP/6-31G(d,p)	-10.0	-2.7	-12.7	10.1	-17.4

d)

Fig. 7. Energy framework of the title molecules viewed along [010], showing: (a) electrostatic, (b) dispersion, (c) total energy force diagrams and (d) the details of interaction with colour-coded, symmetry operation (Symop) and distances between molecular centroids (R) in A.

3.6 DFT calculations

The energy of frontier MOs (FMOs) and the energy gap between them play an important role in chemistry, and they are often used descriptors in the fields of QSAR / QSPR analysis. In addition, frontier electron densities (FED), i.e. the electron density on highest occupied molecular orbital (HOMO) and lowest unoccupied molecular orbital (LUMO) is used to determine, respectively, electrophilic and nucleophilic centers in orbital-controlled reactions.Moreover, the energy of the HOMO is directly related to the ionization potential, while the LUMO energy is directly related to the electron affinity, and the resulting energy difference (or energy gap) between HOMO and LUMO gives information about the stability of a molecule. In the case where the energy gap is small, the molecule is highly polarizable and has a high chemical reactivity.

Calculated numerical values for the title compound, including electronegativity (χ), hardness (η), ionization potential (I), dipole moment (μ), electron affinity (A), electrophilicity (ω) and softness (σ), are collated in Table 3. The electron transition from the HOMO to the LUMO energy level is shown in Fig. 8. The HOMO and LUMO are localized in the plane extending over the whole 4-dimethylaminobenzoylhydrazone of 2,4-dioxopentanoic acid ethyl ester system. The energy band gap [$\Delta E = E_{LUMO} - E_{HOMO}$] of the molecule is 4.522 eV, and the frontier molecular orbital energies, E_{HOMO} and E_{LUMO}, are -5.440 and -0.918 eV, respectively.

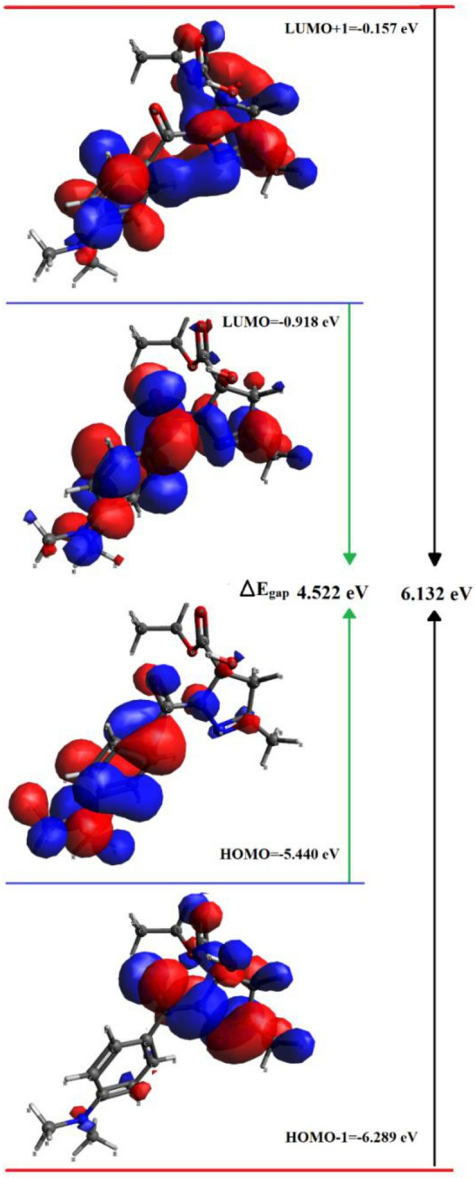

Fig. 8. The energy of FMO and band gap of the (**I**) compound.

Table 3. Quantum chemical parameters for **I** calculated by the DFT/6-31G(d) method in vacuum.

Quantum chemical parameter	(**I**)
E_{HOMO}, eV	-5.440
E_{LUMO}, eV	-0.918
$\|\Delta E\| = E_{HOMO} - E_{LUMO}$, (eV)	4.522
Ionization potentials, $I = - E_{HOMO}$, (eV)	5.440
Electron affinity, $A = - E_{LUMO}$, (eV)	0.918
Electronegativity, $\chi = (I + A)/2$ (eV)	3.179
Chemical hardness, $\eta = (I - A)/2$ (eV)	2.261
Chemical potential, $\mu_p = - (I + A)/2$ (eV)	-3.179
Chemical softness, $\sigma = 1/(2\eta)$ (eV^{-1})	0.22
Electrophilicity index, $\omega = \mu_p^2/2\eta$ (eV)	2.23
Dipole moment, μ (Debye)	6.14

4 Conclusion

In this study, we synthesized and characterized a new hydrazone ligand fater named of the 4-dimethylaminobenzoylhydrazone ethyl ester of 2,4-dioxopentanoic acid. This ligand was confirmed using single-crystal X-ray diffraction (SC-XRD). Analysis of the Hirshfeld surface revealed significant intermolecular interactions contributing to molecular packing within the crystal lattice. Additionally, the relative stability of the HOMO-LUMO frontier orbitals, determined through DFT calculations, suggests the stability of the sample, with discernible differences in breadth between the orbitals. The energy band gap [$\Delta E = E_{LUMO} - E_{HOMO}$] of the molecule is 4.522 eV, and the frontier molecular orbital energies, E_{HOMO} and E_{LUMO}, are -5.440 and -0.918 eV, respectively.

5 Conflict of interest

The authors declare that there is no conflict of interests regarding the publication of this article.

References

1. M. A. Tursunov, B. B. Umarov S. I., Yakimovich, et al., Synthesis and study of para-substituted benzoylhydrazones of 2,4-dioxopentanoic acid ethyl ester. Modern technologies and innovations in the mining and metallurgical industry. NavGGI, Navoi. 14-15 June 2012, pp. 349-350 (2012)
2. S. I. Yakimovich, Tautomeric transformations in a series of nitrogenous derivatives of β-dicarbonyl compounds: Cand. doc. chem. nauk (Leningrad State University, Leningrad, 1988)
3. M. A. Tursunov, B. B. Umarov, Universum: Chemistry and Biology: Electron. Scientific Journal **3(45)**, 45-48 (2018)
4. Weigand-Hilgetag, Experimental methods in organic chemistry. Translation from him. language edited by prof. N.N. Suvorova (Chemistry, Moscow, 1968)
5. A. Gordon, R. Ford, Sputnik chemist (Mir, Moscow, 1974)
6. O. A. Reutov, A. A. Kurts, K. P. Butin, Organic chemistry. Proc. allowance for universities (Publishing House of Moscow State University, Moscow, 1999)
7. Yu. A. Pentin, L. V. Vilkov, Physical research methods in Chemistry (Mir, Moscow, 2003)

8. K. Nakamoto, IR spectra and Raman spectra of inorganic and coordination compounds (Mir, Moscow, 1991)
9. B. A. Ershov, NMR spectroscopy in organic chemistry. St. Petersburg.
10. Xcalibur. Oxford Difraction Ltd. CrysAlisPro. Version.1.171.33.44 (2009)
11. G. M. Sheldrick, Acta Cryst. A71, 3–8 (2015)
12. G. M. Sheldrick, Acta Cryst. C71, 3–8 (2015)
13. C. F. Macrae, I. J. Bruno, J. A. Chisholm, et al., J. Appl. Crystallogr. **41**, 466-470 (2008)
14. M. A. Spackman, D. Jayatilaka, CrystEngComm **11**, 19-32 (2009)
15. F. Neese, Comput. Mol. Science **2**, 73–78 (2012)
16. M. D. Hanwell, D. E. Curtis, D. C. Lonie, et al., J. Chem. Inform. **4**, 17 (2012) DOI: https://doi.org/10.1186/1758-2946-4-17
17. T. Lu, F. ChenJ. Comput. Chem. **33**, 580 (2012)
18. B. B. Umarov, Complex compounds of some transition metals with bis-5-hydroxypyrazolines. Dis.. doc. chem. Sciences (IU ANRUz, Tashkent, 1996)
19. S. I. Yakimovich, V. N. Nikolaev, E. Yu. Kutsenko, Zh. Org.Chemistry **19(11)**, 2333-2339 (1983)
20. S. I. Yakimovich, I. V. Zerova, Zh. Org. Chemistry **27(5)**, 959-965 (1991)
21. M. A. Tursunov, B. B. Umarov , K. G. Avezov, et al., Nauka i Tekhnologii **1**, 158-178 (2012)
22. M. V. Pryadeina, O. G. Kuzueva, Ya. V. Burgart, V. I. Saloutin, Zh. Org. Chemistry **38(2)**, 244-252 (2002)
23. M. A. Tursunov, B. B. Umarov, K. G. Avezov, Moscow University Chemistry Bulletin **74(3)**, 138–142 (2019)
24. M. A. Tursunov, B. B. Umarov, M. Y. Ergashov, et al., J Struct Chem **61**, 73–85 (2020) DOI: https://doi.org/10.1134/S0022476620010084
25. K. G. Avezov, B. B. Umarov, M. A. Tursunov, et al., Russ J Coord Chem **42**, 470–475 (2016) DOI: https://doi.org/10.1134/S1070328416070010